Catena 203 (2021) 105285

Contents lists available at ScienceDirect

Catena

journal homepage: www.elsevier.com/locate/catena

Elucidating suspended sediment dynamics in a glacierized catchment after an exceptional erosion event: The Djankuat catchment, Caucasus Mountains, Russia

Anatoly Tsyplenkov [a,b,*], Matthias Vanmaercke [c], Adrian L. Collins [d], Sergey Kharchenko [a,b], Valentin Golosov [a,b]

[a] Faculty of Geography, Lomonosov Moscow State University, Leninskie Gory, 1, 119991 Moscow, Russian Federation
[b] Institute of Geography, Russian Academy of Sciences, Staromonetny St., 29, 119017 Moscow, Russian Federation
[c] Université de Liège, Département de Géographie, U.R. SPHERES, Clos Mercator 3, 4000 Liège, Belgium
[d] Sustainable Agriculture Sciences Department, Rothamsted Research, North Wyke, Okehampton EX20 2SB, UK

ARTICLE INFO

Keywords:
Sediment yield
Suspended sediment
Hydrological monitoring
Source fingerprinting
Geomorphological mapping
Climate change

ABSTRACT

Suspended sediment yields from glacierized catchments are often among the highest in the world, and their sediment dynamics can be highly variable. This study was undertaken in the 9.1 km^2 glacierized catchment of the Djankuat River located in the Russian part of the Northern Caucasus. The outlet of the study catchment is a hydrological gauging station located at an altitude of 2635 m a.m.s.l. (‘N43°12′31.71″, E42°44′05.93″). The catchment includes a temperate valley glacier (area = 2.42 km^2) and three smaller hanging glaciers, several moraine deposits, rock walls, and a large and expanding proglacial area. The main goal of our study was to assess the impact of an exceptional erosion event on 1st July 2015 (with an annual exceedance probability of less than 0.1%) on suspended sediment yields and the relative contributions of various sediment sources The work combined direct suspended sediment discharge measurements at the gauging station during five ablation seasons (2015–2019) with geomorphic mapping techniques based on detailed field observations and sediment source fingerprinting. Results show that mean annual suspended sediment yields reached 1118 t km^{-2} $year^{-1}$ which is one of the highest measured estimates for any of the glacierized mountain rivers globally. About half of the annual suspended sediment flux was exported during a limited number (1–12% of the annual events) of extreme hydrological events. The sediments mobilized by bank and riverbed erosion within the new lower reach of a tributary channel which appeared after the breakthrough of a lateral moraine became the primary sediment source. It contributed over 50% of the suspended sediment on days with extreme rainfall. Contributions to the suspended sediment load from the glacier source were event-dependent and were only dominant (c. 60–70%) in the upper reaches of the proglacial area (first 800 m). The proglacial part of the study catchment with buried ice was the main sediment source (79%) during non-rain days.

1. Introduction

Climate change is resulting in losses to glacier volumes at an accelerated rate in many high mountain regions (Huss et al., 2008; Huss and Hock, 2018; Shannon et al., 2019; Zemp et al., 2009). This can often lead to erosion and denudation process intensification in glacierized catchments, as reported over the past decade (de Winter et al., 2012). However, because of the glacier-induced basin morphology, much of the eroded sediment can remain stored within such catchments (Hoffmann et al., 2013; Otto et al., 2009). Some potential sinks along the sediment cascade include vegetated talus slopes, lateral moraines, and debris fans (Fryirs et al., 2007; Harvey, 2012). Overall, the sediment connectivity between hillslopes and stream channels depends on both the characteristics and arrangement of the different geomorphic units as well as on the erosion and sediment transport processes taking place (e.g., Messenzehl et al., 2014). Air temperature and precipitation are two key parameters that have influenced the intensity of these processes in the proglacial zones of mountainous catchments (Lane et al., 2017; Stott and Mount, 2007). Local, but intense, thunderstorms can generate events with high peak runoff discharges and suspended sediment

* Corresponding author at: Faculty of Geography, Lomonosov Moscow State University, Leninskie Gory, 1, 119991 Moscow, Russian Federation.
E-mail address: atsyplenkov@geogr.msu.ru (A. Tsyplenkov).

https://doi.org/10.1016/j.catena.2021.105285
Received 9 July 2020; Received in revised form 8 February 2021; Accepted 27 February 2021

concentrations that are responsible for most of the sediment export from small high mountainous catchments (Navratil et al., 2012). In addition to rainfall-driven floods, glacier lake outburst floods and glacier floods are common in alpine environments (e.g., Carrivick and Tweed, 2016). Such extreme events often play a crucial, yet complex, role in redistributing sediments within proglacial zones (e.g., Cenderelli and Wohl, 2001; Cook et al., 2018; Richardson and Reynolds, 2000; Warburton, 1990; Wilson et al., 2019). Quantifying and understanding these dynamics is not only of great relevance from geomorphological and hydrological perspectives; it is also crucial for better predicting and managing catchment sediment dynamics and associated potential societal impacts, such as the siltation of hydropower reservoirs situated downstream (e.g., Owens et al., 2005). This is especially so in the current context of climate change and its associated impacts on glacierized catchments that are a key source of water to larger drainage systems.

Previously studies reported that the proglacial zones of catchments in the Caucasus mountains are characterized by high denudation rates (Tsyplenkov et al., 2019; Vezzoli et al., 2020), often as a result of recent extreme events (Chernomorets et al., 2018; Evans et al., 2009; Haeberli et al., 2004). Nevertheless, our insights into the relative role and importance of different sediment sinks and sources in these glacierized catchments and their sensitivity to climate change remain limited (e.g., Yermolaev et al., 2015). The first reason for this is the relatively limited availability of measurements quantifying water and sediment yields from such catchments over time (Lewis et al., 2005; Tsyplenkov et al., 2020). Secondly, the geomorphic complexity of glacierized catchments and their sediment dynamics make it challenging to assess and compare the relative contributions of glacial and non-glacial sediment sources to catchment sediment yields (Harbor and Warburton, 1993).

Detailed monitoring of suspended sediment fluxes over time is key to quantifying the total rates of catchment-wide denudation and the associated temporal dynamics (Leggat et al., 2015; Micheletti and Lane, 2016). However, while conventional hydro-sedimentological data provide evidence of integrated catchment responses, they cannot disentangle the importance of different sediment sources (Tsyplenkov et al., 2020). However, sediment source fingerprinting can offer a basis for evaluating the relative contributions of various sediment sources (Collins et al., 1997; Collins and Walling, 2004). The first studies on quantifying the relative contributions of different sediment sources to the sediment yields of catchments in polar and high mountain regions were undertaken during the 1990s (Gurnell, 1995; 1987; Hasholt et al., 2000; Hasholt and Walling, 1992). However, since then, very little work has been undertaken using the fingerprinting approach for identification of the contributions of various sediment sources in glacierized catchments. The broader context of a changing climate and its impacts on extreme events make the need for such insights more pertinent.

Quantitatively linking fingerprint properties or tracers in target sediment samples (e.g., those collected from the suspended load, riverbed or floodplain) to those in upstream sources is often very challenging due to non-conservative behaviour (e.g., exchanges between the dissolved and particulate phase) during sediment transport (Collins et al., 2017, 1997; Guzmán et al., 2013; Koiter et al., 2013; Sear et al., 2002; Walling, 2005). Numerous chemical, biological and physical processes can alter sediment properties as particulate material moves along the sediment cascade (Koiter et al., 2013; Mabit et al., 2008; Smith and Blake, 2014). Robust source fingerprinting therefore requires the use of tracers that remain conservative during their transport along the pathways from source to sink.

In addition, the successful application of sediment fingerprinting also depends on a meaningful classification of potential sediment sources. As such, geomorphic mapping using fieldwork and GIS analyses can offer complementary insights on the provenance and redistribution of sediments within catchments at a more detailed scale (Collins and Walling, 2004; Heckmann et al., 2016; Heckmann and Schwanghart, 2013; Messenzehl et al., 2014). Nevertheless, classical geomorphological maps alone are generally insufficient for fully characterizing glacierized catchments. One reason for this is that related landforms may change very quickly over short distances and timescales (Heckmann and Schwanghart, 2013). Furthermore, geomorphological maps generally remain qualitative. To some extent, modelling sediment connectivity, based on detailed DEMs and other remote sensing data, can help in quantifying certain aspects of sediment transfers (Cavalli et al., 2013; Laute and Beylich, 2014; Wichmann et al., 2009). However, their correct interpretation is often challenging (e.g., Messenzehl et al., 2014).

Each of the techniques mentioned above has shortcomings, challenges, and advantages. As such, combining measurements of catchment sediment export with sediment source fingerprinting (e.g., Navratil et al., 2012), geomorphic mapping (Heckmann and Schwanghart, 2013; Messenzehl et al., 2014; Theler et al., 2010) and conventional suspended sediment monitoring (Leggat et al., 2015; Micheletti and Lane, 2016) offers potential to quantify better and understand the dynamics and sources of sediments in complex glacierized catchments. Combination of such research methods offers a weight-of-evidence approach which can help mitigate the limitations associated with the application of any individual method.

Accordingly, the primary purpose of this study was to understand and quantify the sediment dynamics and sources within the Djankuat River, a glacierized catchment in the Northern Caucasus mountains, over a period spanning several years after an exceptional erosion event that occurred on 1st July 2015. This event was associated with heavy rainfall, amounting to a total precipitation of 227 mm in one week. The extreme event led to a breakthrough of the Djankuat glacier lateral moraine on the right side of the valley and the formation of the new lower reach of the Koiavgan Creek, a tributary of the Djankuat River (Rets et al., 2019; Kharchenko et al., 2020). It is plausible that such an extreme event could influence the Djankuat River sediment yield and the relative contributions of different sediment sources. As such, we aimed to provide more insight into the relative importance of such an exceptional event for sediment dynamics over consecutive years. More specifically, our research objectives were:

- To quantify the sediment fluxes and their temporal variation in the Djankuat catchment over five ablation seasons following an extreme event.
- To assess the impacts of extreme rainfall events on the sediment flux of the Djankuat catchment.
- To identify the main sediment sources within this glacierized catchment and evaluate their overall contribution to suspended sediment loads during different hydrological events.

2. Study site

The 9.1 km^2 catchment of the Djankuat River (Fig. 1) is located in the Russian part of the Northern Caucasus, near the Russian-Georgian border. The outlet of the study catchment is a hydrological gauging station ('OUT' in Fig. 1; N43°12′31.71″, E42°44′05.93″, altitude: 2635 m a.s.l.). The catchment includes a temperate valley glacier (called the Djankuat glacier), with a surface area of 2.42 km^2. The Djankuat glacier belongs to the central section of the Glavny (Main) ridge of the Greater Caucasus, with altitudes ranging between 2700 and 3900 m a.s.l. (Shahgedanova et al., 2007). Regular mass-balance measurements began in 1967. Currently, Djankuat is monitored by the World Glacier Monitoring Service as one of the world's ten representative glaciers (Dyurgerov, 2003; Shahgedanova et al., 2007). The study catchment further includes three smaller hanging glaciers, several moraine deposits (some of which remain ice-cored), rock walls, and a large and expanding proglacial area. Overall, the surface geology is composed of Galdorian metamorphic rocks (migmatites, gneisses) with sparse Ullucamian plutonic pegmatites associated with faults (Pismenniy et al., 2013). The average scale of available geological maps does not allow us to judge the spatial heterogeneity of the composition of pre-Quaternary rocks exposed at the surface. Nevertheless, morphological features of the relief

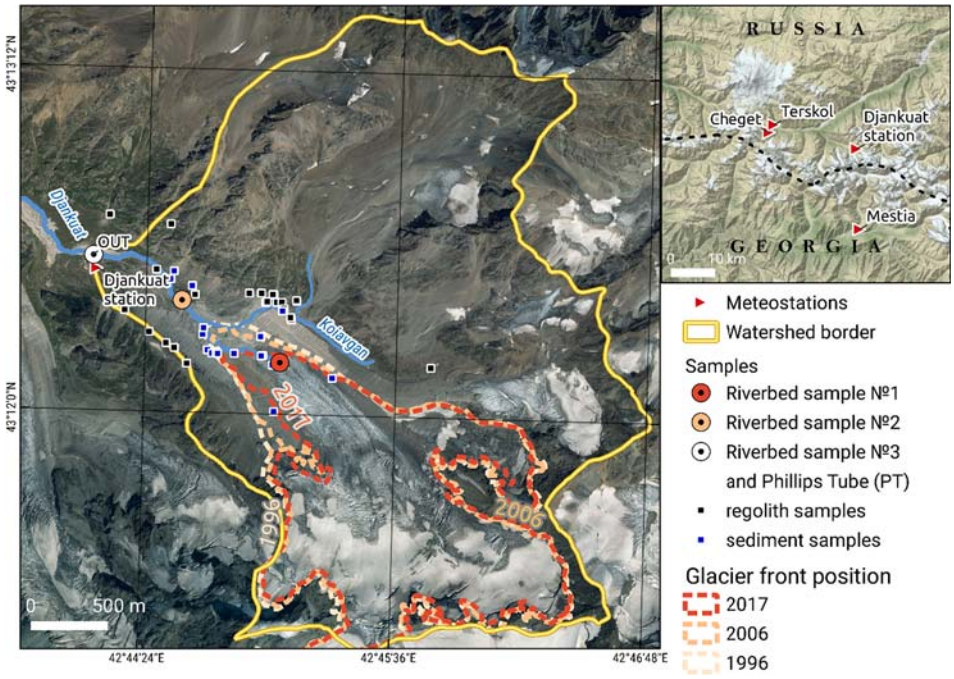

Fig. 1. Overview of the Djankuat catchment showing the extent of the main glacier, the positions of the gauging stations, and the riverbed and source sampling sites used for the sediment fingerprinting. The background image is a WorldView-2 Satellite Image from August 2010.

suggest certain differences in the degree of disjunctive disturbances and the intensity of bedrock weathering. This indicates some differences in lithological composition. The Quaternary sediment cover is represented by moraines of different ages, talus, eluvium and deluvium sediments on the bedrock surface and, to a lesser extent, fluvial and fluvioglacial sediments (see SM1 for details on the geomorphological features of the Djankuat catchment).

According to meteorological observations for 2007–2019, the average daily precipitation depth (in rainfall equivalents) is 11.2 mm per day (mean for the days with liquid precipitation), with a corresponding maximum of 97.2 mm per day (Rets et al., 2019). Most of the precipitation falls during the cold season (October–May) as snow. Air temperatures during the ablation period (May-September) range from −1.1 to 24.2 °C, with an average of 10.2 °C at the monitoring station and between −9 and 17.6 °C (mean of 6.6 °C) at the glaciers (about 3000 m a.m.s.l.). Overall, the study catchment is covered with snow from October until late May–early June. At the beginning of July, only a few patches of snow remain at the highest elevations and on north-facing slopes of the non-glaciated area.

Typically, the river is frozen during the winter (October–May) (Rets and Kireeva, 2010). As a result, around 98% of the total runoff and sediment discharge occurs during the ablation period (Durgerov et al., 1972; Rets et al., 2017). Mean water discharge for the ablation period at the outlet (OUT) of the study catchment is 1.38 $m^3 \cdot s^{-1}$. On days without intensive rainfall, water discharge during the ablation season ranges between 1 and 2 $m^3 \cdot s^{-1}$ (Rets et al., 2019). Peak water discharges are associated with heavy rainfall events and can reach up to 3–4 $m^3 \cdot s^{-1}$. Such events are most frequently observed in the second half of the ablation season (Rets et al., 2019). Rets et al. (2017) estimated that snow and ice-melting processes are the main sources of water discharge (44%), followed by groundwater flow (37%) and surface runoff during rainfall events (19%).

3. Materials and methods

A combination of different methods and approaches were used to understand the effects of the exceptional erosion event on the sediment yield of the Djankuat catchment over the period 2015–2019 and the contributions of different sediment sources. We used conventional hydrometeorological measurements including water and sediment discharges (at the OUT station, see Fig. 1 for location) and meteorological observations (precipitation) during the ablation seasons of 2015–2019. Furthermore, the main sediment sources were identified based on the analysis of the geomorphological features of the different subcatchments of the Djankuat River catchment and we evaluated the relative contributions of the primary sediment sources to sediment flux using the source fingerprinting approach.

3.1. Hydrometeorological and suspended sediment measurements

Water discharge for the Djankuat River was calculated from the water level using a rating curve $Q = f(H)$. The water level was recorded with a 10 min to hourly time step, using a Solinst Levellogger Junior. Additionally, manual water level measurements were taken six to seven times a day at the OUT gauging station (Table 1; see Fig. 1 for location). Rating curves were constructed for each month annually (Rets et al., 2019). Water discharge was measured via dilution, using NaCl as a tracer. Dilution was performed for discharge measurements as turbulent flow conditions make it impossible to apply a current meter (Dobriyal et al., 2017).

Turbidity measurements were performed manually using a portable turbidity meter (Hach 2100P). During heavy rainfall events, the

Table 1
Characteristics of the OUT gauging station and periods of observation for ablation seasons (2015–2019).

Station code (see Fig. 1 for location)	OUT
Catchment area, km^2	9.1
River length, km from the glacier snout	1.62
Period of observation	2015 – 2019*
Minimum elevation, m	2648
Maximum elevation, m	3848
Elevation range, m	1200
Glacierized area, %	27

* 08.06.2015–19.09.2015; 09.06.2016–19.09.2016, 03.06.17–25.09.17, 03.06.18–27.09.2018, 06.06.2019–21.09.2019.

measurements were performed every 15 min. Additionally, water samples were taken manually under various turbidity conditions and filtered using 0.45 μm Millipore membrane filters to compute suspended sediment concentrations (SSC [g m^{-3}]) (Rets et al., 2019). The suspended sediment concentrations and turbidity have been measured since 2015 (six to seven times a day) at the OUT gauging station during the ablation season (May-September). Air pressure, temperature, and other meteorological characteristics were monitored at OUT using a Davis AWS (Rets et al., 2019). Precipitation depths were measured manually for every rainfall event since 2015. The rain gauge was located 0.5 m above ground. A more detailed description of the hydrological and meteorological measurements is presented in Rets et al. (2019). The methodological aspects of the turbidity (*T*, NTU) and suspended sediment concentration (*SSC*, g·m^{-3}) measurements are described in detail in Tsyplenkov et al. (2020).

We aimed to quantify the sediment export on an event-basis over multiple years and to quantify the relative importance of different sediment sources within the study catchment. For this, we first demarcated all hydrological events. This was done by smoothing the hourly water discharge values (Q_{OUT}) using a linear moving median function with a window size of three hours (as suggested by Rodda and Little, 2015) and identifying the start and endpoint of each event, using the local minimum method (Sloto and Crouse, 1996) within a 24-hours window (see Tsyplenkov et al. (2020) for further details).

For each demarcated event at the OUT station, we calculated the suspended sediment load as:

$$SSL_i = \frac{\sum_{k=1}^{n} Q_k \hat{\mathrm{A}}\cdot SSC_k}{n\hat{\mathrm{A}}\cdot 10^6}\hat{\mathrm{A}}\cdot\Delta t, \quad (1)$$

where SSL_i is the suspended sediment load [t $event^{-1}$] for event *i*; Q_k is the measured or estimated water discharge at the time *k* [m^3 s^{-1}]; SSC_k is the corresponding measured suspended sediment concentration at the time *k* [g m^{-3}]; *n* is the number of pairwise (*Q* and *SSC*) measurements taken during that event, and; Δt is the duration [s] of the hydrological event. Therefore, suspended sediment flux for the ablation season [t] can be calculated as the sum of SSL of all events during the observation period. The total annual suspended sediment flux was estimated as 1.02 times the suspended sediment flux during the ablation season (corresponding to the estimate that 98% of the total annual sediment and water discharge occurs during the ablation period (Durgerov et al., 1972; Rets et al., 2017)).

According to terminology used in sediment transport studies (e.g. Lana-Renault et al., 2014; Lizaga et al., 2019; Rainato et al., 2017), the event that occurred on 1st July 2015 (discussed in the Introduction) was 'exceptional'. Other large or significant hydrological events we called 'extreme'. Quantitively, extreme events were those whose cumulative ranked suspended sediment loads (i.e., ones with the largest SSL) were more than half of the annual total.

3.1.1. Assessing daily and weekly rainfall event frequency

Since both hydrological and meteorological measurements at the Djankuat catchment are limited to a 12-year observation period (2007–2019), we estimated the overall return periods of events using data from the nearest meteorological stations: Terskol, Cheget and Mestia (Table 2, cf. Fig. 1 for locations). The daily and rolling 7-day precipitation sums were calculated for every station. We used a +2.0 °C rain-snow temperature threshold (i.e., the 50% rain-snow air temperature threshold estimated by Jennings et al. (2018)). An R package routine (Goetz and Schwarz, 2020) was used to determine the frequencies of daily and weekly maximum rainfall depths. The probabilities (*P*) of each event were determined using the following equation:

$$P = \frac{m}{n+1}, \quad (2)$$

where *m* is the rank of the value and *n* is the total number of events in the dataset. We also computed frequency quantiles by fitting the data to a Pearson Log III distribution using the method of moments.

3.2. Preliminary identification of the main sediment sources and assessment of their contributions to the Djankuat River sediment yield

3.2.1. Identification of sediment sources

Conceptually, the exceptional erosion event discussed in the Introduction might influence the sediment contributions from different parts of the Djankuat River catchment. This is because of the large volume of material that was mobilised and the substantial sediment cone which appeared at the bottom of the Djankuat valley in the area of the lateral moraine breakthrough (see Fig. 2).

The incision of the Koiavgan Creek channel began in the lower reach due to the breakthrough (Kharchenko et al., 2020). The former lower reach of the Koiavgan Creek joins the main stream of the Djankuat River about a few hundred meters downstream (see Fig. 2).

The results of field observations and a geomorphological map of the Djankuat catchment (see SM1) were used for the initial identification of the main potential sediment sources. The Djankuat glacier and two sub-catchments adjacent to the glacier on the left and right side were identified as the key first potential sediment sources, because of the continuous water flow during the ablation season from these areas. The Koiavgan Creek catchment (the tributary of the Djankuat River, see Fig. 1) accounts for almost half of the Djankuat catchment. It consists of two sub-catchments, which are characterized by similar morphological features. Their peripheral parts are zones of active rockfall and scree processes, whereas the central parts are expansive areas for the redeposition of clastic and moraine material. The Koiavgan Creek catchment up to the confluence of the two streams was identified as a second potential sediment source. The lower reach of the Koiavgan Creek channel is the boundary between two other potential sediment sources, which were named "Right bank" and "Buried ice". The "Buried ice" area incorporates parts of the right and left banks of the Djankuat valley adjacent to the glacier snout, which is characterized by the high amount of ice buried under the moraine and talus deposits. This part of the catchment was part of the glacier in 1996 (see glacier boundary location in 1996 on Fig. 1). The part of the right bank of the Djankuat river valley, located downstream of the Koiavgan Creek channel (see SM1) is a separate potential sediment source, which consists of a few small sub-catchments. This is an area with partly vegetated very steep slopes with many bedrock outcrops dissected by erosional landforms (e.g., rills and micro-rills). Also the part of the left bank of the Djankuat River valley, which is located at a distance from the front of the glacier, can be considered as an independent potential sediment source (Fig. 3). It is a lateral moraine without vegetation cover, dissected by a dense system of rills. In summary, five preliminary potential sediment sources were selected (Fig. 3). The source fingerprinting approach was used to

Table 2
Meteorological data used in this work.

Station	WMO ID[1]	Geographical coordinates	Elevation, m a.s.l.	Distance from Djankuat catchment, km	Observation period	Mean annual rainfall, mm
Terskol	37,204	43°15′N,42°30′E	2140	18	1977–2020	607
Cheget	37,205	43°23′N,42°51′E	3040	19.4	2007–2020	452
Mestia	37,209	43°05′N,42°72′E	1441	18	1966–1992	376

[1] World Meteorological Organization station number.

Fig. 2. View of the upper reach of the Djankuat River and the large sediment cone which appeared after the breakthrough of the lateral moraine on the 1st July 2015. The glacier snout is visible at the right edge of the photo and the former Koiavgan lower reach on the left side of the image (Photo from an unmanned aerial vehicle, DJI Mavic PRO, September 2019).

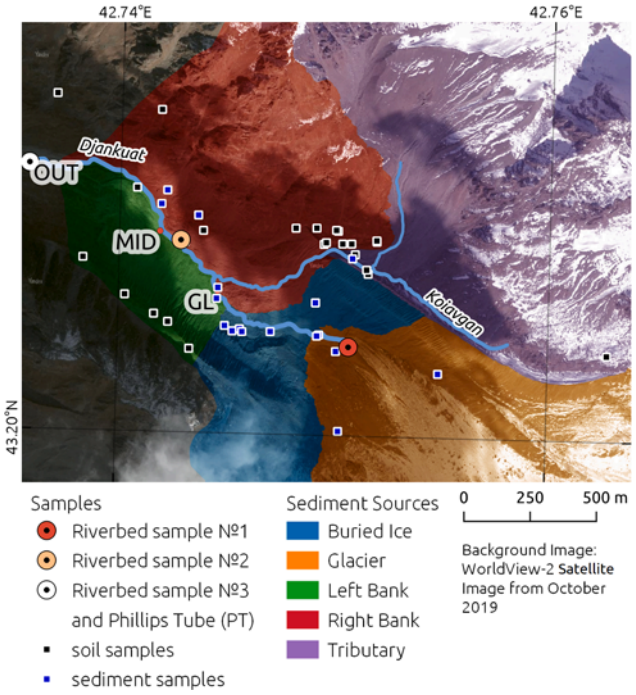

Fig. 3. Main potential sediment sources in the Djankuat valley and corresponding sampling points.

provide a preliminary assessment of the relative contribution of these different potential sources to the sediment yield of the Djankuat catchment along the stream reach from the glacier snout to the gauging station at OUT (Fig. 1).

3.2.2. *Sampling site selection for source fingerprinting*

The source fingerprinting work necessitated the collection of source soil and target sediment samples (Fig. 3). Different approaches were used for the selection of representative sampling sites for the different potential sediment sources. The first group of sediment sources, including "Glacier" and "Tributary" (Fig. 1) are characterized by large areas with difficult access to the upper parts of their tributaries. Accordingly, the sampling sites for these potential sources were selected in areas with redeposition of fluvial or glacio-fluvial sediments. Material sampled at these sites was assumed to provide a spatially-integrated signature for the possible source in question. Access was less of an issue for the remaining sources.

Sampling sites for surface regolith in the Djankuat catchment were selected based on some general criteria: (i) proximity to, and connectivity with, streams, and; (ii) possible evidence of the erosion of slopes based on partial vegetation cover or bare ground. Sampling sites on the barren slopes were distributed across the entire area in question (i.e., "Left bank" and "Buried ice" potential sediment sources). Regolith samples on the vegetated slopes that were more characteristic of the "Right bank" potential source were taken along a slope transect. Sampling locations in the "Right bank", "Left bank" and "Buried ice" sources were mainly located in the corresponding sediment cones. Each source material sample comprised a composite of smaller scrapes collected at 4–5 points to increase the representativeness of the individual sample (Collins et al., 2017; Lizaga et al., 2019). Regolith and sediment samples were taken from a depth of 0–3 cm at most sampling sites. In some cases, due to the large amount of coarse material, samples were taken from a depth of 0–5 cm.

To examine the relative contribution of the different potential sources to the Djankuat River sediment yield four years after the exceptional event of 2015, surface scrapes of exposed riverbed sediments were collected from the drainage channel at three locations (Fig. 3). Samples were collected from a single bar in the channel at each location using a shovel. This was done to sample material assumed to be freshly deposited during the falling limb of the most recent flood. Since

exposed bed sediment deposits were sampled, there was no need for the use of the more conventional stilling well remobilization method, which is widely applied in fluvial environments to avoid the winnowing of fines when submerged bed sediments are disturbed by the collection of samples (Lambert and Walling, 1988). The locations of riverbed sampling sites were selected along the main Djankuat River channel to reflect an increasing number of potential sediment sources with scale (cf. Fig. 3).

Suspended sediment was collected at sampling point 3 (OUT gauging station) (Fig. 1) using an in-situ time-integrated sampler, based on the design outlined by Phillips et al. (2000). The time-integrated sampler was installed for 24 h (ca. the duration of one hydrological event in the non-rain day period) for collecting a suspended sediment sample. We hypothesized that it represents a typical hydrological event without the contribution of surface runoff from the catchment slopes due to effective rainfall.

All soil and bed sediment scrape samples were returned to the laboratory, oven-dried at 105 °C, manually disaggregated using a pestle and mortar, and dry sieved to 63 μm. The 63 μm limit was selected since it has been successfully used in many source fingerprinting studies (Collins et al., 2017; Gaspar et al., 2019a; Lizaga et al., 2019; Owens et al., 2016). Water and sediment captured by the time-integrated sampler were extracted in the field into a container and stored in a cold room for 24 h. This allowed settling and siphoning of the clear supernatant water. The remaining sediment–water mix was centrifuged at 3000 rpm for 20 min and the supernatant decanted. The sediment sample was freeze-dried for 48 h, then gently disaggregated and sieved to <63 μm for analysis to permit direct comparison with the source material samples. The analyses of elemental geochemistry were performed at the A.N. Severtsov Institute of Ecology and Evolution following the ISO/TS 18705:2015 procedure. 200–500 mg sub-samples were dissolved in a MARS 5 microwave high-pressure oven ("CEM Corp.") at a maximum pressure of 800 psi at 240 °C. Next, they were analyzed by X-Ray Fluorescence (XRF) using a PicoTax TXRF spectrometer ("Bruker AXS"). The analytical uncertainty for the geochemistry measurements was less than 5–10%. Source and target sediment samples were analyzed for major and minor elements (Mg, Al, Si, P, S, K, Ca, Ti, Cr, Mn, Fe, Co, Ni, Cu, Zn, As, Rb, Sr, Ba, W, Hg, Pb, Bi, Sn, Sb, Zr, Hf, Sm, Ho, Nd, Se, Ga, Au, Th, U, Cl, Tl, Ta, Nb). Only those elements returning measurements above the limit of detection were used in the data analysis for source fingerprinting.

3.2.3. Sediment source discrimination and apportionment

The discrimination of the potential sediment sources and the preliminary estimation of the relative contribution of each source to the sampled river sediment was performed using the FingerPro software (Lizaga et al., 2018). A 4-step selection of tracers was made before an un-mixing model was run, following recommendations from previous studies and model manuals (Collins et al., 1996; Lizaga et al., 2019; Walling, 2005). First, we checked for multicollinearity in the tracer data (based on a Spearman's rank correlation test) and deleted collinear geochemical elements. Second, we then compared the tracer ranges in the sediment sources to the corresponding ranges in the target sediment samples to assess tracer conservation. Third, we used a non-parametric Kruskal-Wallis *H*-test to remove those tracers that do not show a significant (p-value $>$ 0.05) difference between the potential sediment sources (Collins et al., 1996). Finally, a stepwise multivariate discriminant function analysis was applied to the list of conservative tracers that were selected in the previous step to identify a final composite signature for source discrimination and for shortlisting the tracers for inclusion in the un-mixing model (Collins et al., 1996).

The structure of the standard linear multivariate un-mixing model is explained in Gaspar et al. (2019a). This model uses Monte Carlo random sampling of source material tracer distributions to determine the deviate relative contributions from the different sediment sources. Although the use of FingerPro is gradually increasing (Gaspar et al., 2019b; 2019a; Lizaga et al., 2019), to date, there have been no applications of this software in a case study involving a glacierized catchment. To assess the ability of the un-mixing model to predict the measured tracer concentrations in the target sediment samples, we used the goodness-of-fit (GOF) criterion suggested by Motha et al. (2003). Application of this GOF estimator is very common in fingerprinting studies (Evrard et al., 2011; Lizaga et al., 2019; Palazón et al., 2015; Pulley and Collins, 2018). It calculates the root mean square of relative errors between the predicted and actual tracer concentrations and is implemented in the FingerPro software.

4. Results

4.1. Exceptional and extreme erosion events and suspended sediment yield dynamics during 2015–2019

Since there is a limited period of meteorological observations at the Djankuat River, we used rainfall data collected from nearby meteorological stations to assess the frequency of large events that occurred. The frequency plots for maximum daily and maximum weekly rainfalls are presented in Fig. 4a and b.

The breakthrough of the Djankuat glacier lateral moraine on the right side of the valley occurred on the 1st July 2015 after continuous rainfall which yielded a 7-day total of 227 mm (Rets et al., 2019). The annual exceedance probability (AEP) of this weekly rainfall total is <0.1% (cf. Fig. 4b). More specifically, 87.1 mm of the precipitation fell in four days between 25th and 28th June 2015. This is 90% of the monthly average for the Djankuat catchment (for the period 2007–2019). On 29th June 2015, an additional 50 mm of rain fell with a corresponding AEP of ca. 20%. This caused a significant increase in water discharge: around 3:00 AM on 30th June 2015, water discharge increased to 8.3 $m^3 \cdot s^{-1}$. On 30th June 2015, another 56 mm of rainfall (AEP ≈ 13–15%) was recorded. This resulted in a breakthrough of the right-bank moraine by the Koiavgan stream after midnight and a water discharge peak of 8.46 $m^3 \cdot s^{-1}$ at 9:00 on 1st July 2015. The total estimated suspended sediment export after the breakthrough was ~9500 t (Kharchenko et al., 2020). In the next 24 h (July 1st), another 33 mm of rainfall (AEP ≈ 66–88%) was recorded. In total, therefore, around 227 mm of rain was recorded that week, which is 2.3 times the monthly average (Kharchenko et al., 2020). As a result, an estimated 156 000 m^3 of sediment was exported to the bottom of the Djankuat River valley. The majority of this sediment was deposited in the sediment cone, which was situated at the location of the Koiavgan Creek delta (Fig. 2). (Kharchenko et al., 2020).

Unfortunately, it was not possible to measure the total amount of sediment exported from the study catchment during this *exceptional* event, because the gauging station was damaged during the flood associated with the breakthrough of the lateral moraine. This occurred at midnight, and observations only restarted at 9:00 AM. An undetermined portion of the sediment discharge between the moment of the breakthrough and the restoration of hydrological observations was therefore not measured. Hence, the suspended sediment load data presented in Table 3 are most likely underestimated for the ablation season of 2015.

Before the moraine breakthrough, water discharge increased to 8.30 $m^3 \cdot s^{-1}$ and 7.58 $m^3 \cdot s^{-1}$ (29th and 30th June 2015, respectively). At the same time, suspended sediment concentrations increased only to 2628 $g \cdot m^{-3}$ and 4828 $g \cdot m^{-3}$, respectively.

Another extreme flood was observed on the 1st of September 2017, when the maximum SSC for the study period (2015–2019) was measured (Table 3). This flood was associated with a total precipitation of 87 mm per day and a corresponding maximum intensity of 33 mm per hour. The AEP of this rainfall event is <1% (cf. Fig. 4a). Again, our hydrological gauge was partly destroyed, and a portion of the sediment flux was not measured. However, at least 1800 t of sediment (19% of the total suspended sediment load during the corresponding ablation

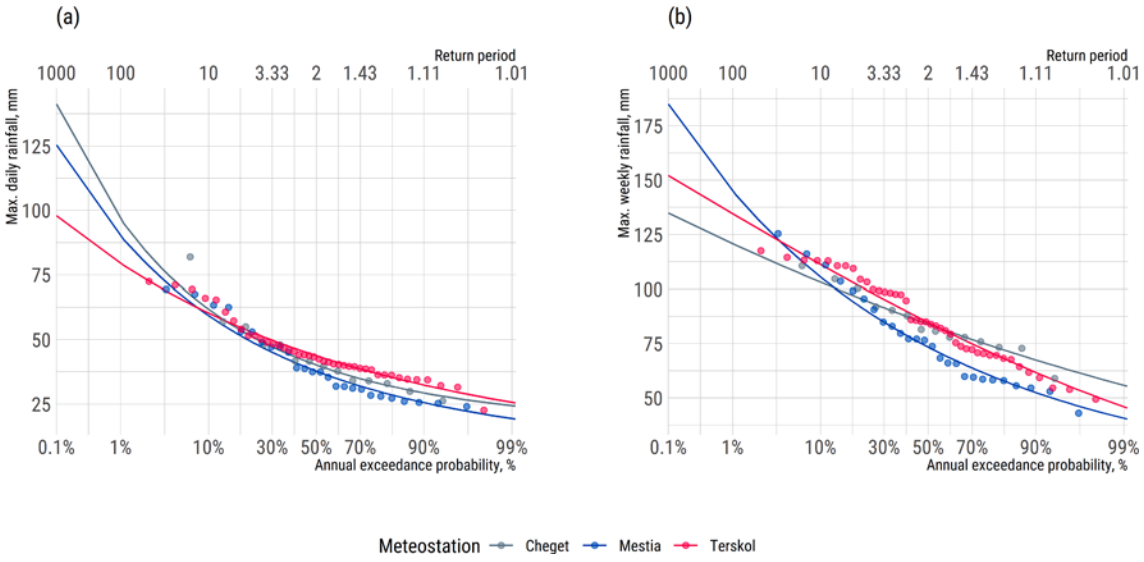

Fig. 4. Annual exceedance probabilities of maximum daily (a) and weekly (b) rainfalls based on data from the Cheget, Mestia and Terskol meteorological stations (see Fig. 1 for locations).

Table 3
Suspended sediment loads (SSL_{OUT}) and concentrations (SSC) at the outlet gauging station (OUT) of the Djankuat study catchment (cf. Fig. 1) for the period 2015–2019.

Year	*SSL* during the observation period[1] [t]	Estimated annual *SSL*[3] [t]	SSL_{Mean} [t·event^{-1}]	St. Dev. [t·event^{-1}]	SSL_{Med} [t·event^{-1}]	SSL_{Max} [t·event^{-1}]	SSL_{Min} [t·event^{-1}]	SSC_{med} g·m^{-3}	SSC_{Max} g·m^{-3}	Time of SSC_{Max}
2015	22,010[2]	22,450	158	817	46	9500	1.1	266	43,344[2]	1st July 2015 09:00
2016	8290	8455	63.3	100	33	600	1.7	252	8851	5th August 2016 20:00
2017	9224[2]	9408	68.3	170	30	1800	1.9	237	53,788[2]	1st September 2017 03:00
2018	5482	5591	46.8	229	21	2500	4.1	218	4220	10th September 2018 11:00
2019	4866	4963	33.6	150	13	1800	0.24	218	23,420	24th June 2019 10:15

[1] Period of observation from the beginning of June till the end of September.
[2] Underestimated due to interruption of water level and turbidity observations during extreme flood events.
[3] Estimated as 1.02 times greater than SSL during the observation period.

season) was removed from the Djankuat catchment during this event. It is likely that most of the high sediment load occurred due to the mainly fine sediment eroded by the stream of the Koiavgan Creek in the breakthrough and from the sediment cone (Fig. 5).

One more extreme event was recorded in July 2018. As a result of several rainfall events with a total of 159 mm per 7-days, 2520 t of suspended sediment was exported (corresponding to 46% of the annual load in 2018). The maximum water discharge was relatively low — only 3.81 m^3·s^{-1}, while the maximum measured SSC reached 3549 g·m^{-3}.

During 2015–2019 there were, on average, 130 hydrological events per ablation season in the Djankuat study catchment. The mean suspended sediment load (SSL_{OUT}; cf. Eq. (1)) was estimated to be 69.4 t·event^{-1} (Standard Deviation: 381 t·event^{-1}), with a corresponding median of 25.6 t·event^{-1}. A clear trend of declining annual suspended

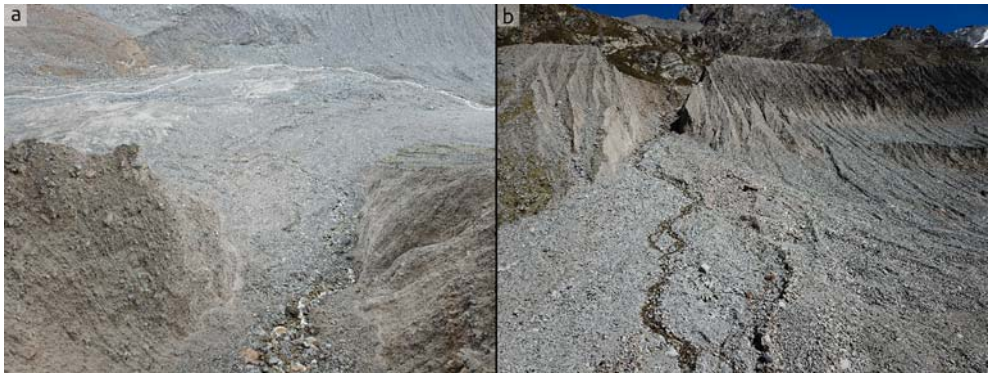

Fig. 5. Views of the breakthrough in the lateral moraine (September 2019): (a) from the side of the breakthrough, and; (b) from the Djankuat River valley side.

sediment loads was observed for the period 2015–2019 (Table 3). The mean annual suspended sediment flux was estimated at 10,174 t·yr^{-1}, corresponding to an equivalent specific suspended sediment yield of 1118 t·km^{-2}yr^{-1}. However, the actual suspended sediment yield was most likely higher due to interrupted measurements during two extreme floods in the study period.

We found that the majority of the annual suspended sediment loads were exported by a limited number of hydrological events (Table 4). The occurrence and magnitude of these events were associated with intense rainfall, which led both to increased snow and glacier melting and surface runoff from other parts of the Djankuat catchment (Rets et al., 2017).

For the whole measurement period (2015–2019), around 50% of the total sediment load at the OUT station was transported during the largest 2–16 recorded events (ca. 5% of the annual event amount on average). In other words, ~50% of the annual suspended sediment load was exported during hydrological events caused by 32–44% of the seasonal rainfall (Table 4). This is most likely an underestimation as measurements were interrupted during the exceptional event in 2015.

4.2. *Preliminary estimation of the contribution of the different sediment sources using fingerprinting*

Linear discriminant analysis (LDA) in the FingerPro software revealed an overlap between the "Buried Ice" and "Left Bank" potential sources (Fig. 6). This was generally expected, given that they have a similar genesis (lateral moraine). Thus, "Buried Ice" and "Left Bank" were grouped as one potential sediment source ("Buried Ice").

The 4-step selection of tracers allowed us to select a final composite signature consisting of Mg, Ca, Zn, Rb, W, and Hg. However, due to the high variability of Rb in the riverbed, glacier, and tributary samples, we decided to exclude it. Summary statistics for the shortlisted tracers in the final composite signature are presented in Table 5.

The final four potential sediment sources were identified as: "Glacier", "Tributary", "Right bank" and "Buried Ice". The fingerprinting approach was used to estimate contributions of these sediment sources along the river channel from the glacier snout to the OUT gauging station (Table 6). Substantial variations in the estimated contributions from the various sediment sources were evident for each riverbed sediment sample (Fig. 7).

The time-integrated suspended sediment sample (PT) was taken during a typical hydrological event for a non-rainy day. The "Buried Ice"

Table 4
Summary statistics of the extreme events[1] during the 2015–2019 observation period.

Year	2015	2016	2017	2018	2019
Number of recorded hydrological events	139	131	135	117	145
SSL during observation period[2,3] [t]	22,010	8290	9224	5482	4866
Number of extreme events [1]	2	16	10	3	6
Number of extreme events as a percentage of total recorded hydrological events[1] [%]	1%	12%	7%	3%	4%
Contribution of extreme events to annual *SSL* [t]	11,000	4210	4540	2758	2434
Contribution of extreme events to annual *SSL* [%]	50	51	49	50	50
Rainfall totals corresponding to extreme events [mm]	–	159	156	234	–
Rainfall totals per ablation season [mm]	464	455	482	534	–
Extreme event rainfall as a proportion of the total rainfall per ablation season [%]	–	35%	32%	44%	–
Annual suspended sediment yield[3] [t km^{-2} yr^{-1}]	2467	929	1033	614	545

[1] The total sum of which exceeds 50% of the annual suspended sediment load.
[2] Observation periods spanned from the beginning of June until the end of September.
[3] See Table 3 for the estimated SSL.

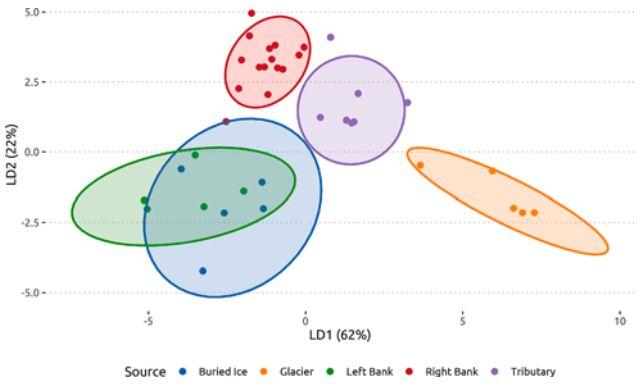

Fig. 6. LDA plot of the different potential sediment sources in the Djankuat study catchment.

Table 5
Summary statistics for the tracers shortlisted in the final composite signature.

Source	Element	Mean	St.Dev	Median	Max	Min
Glacier	Ca [g kg^{-1}]	2.31	0.498	2.17	3.11	1.89
	Hg [g kg^{-1}]	0	0	0	0	0
	Mg [g kg^{-1}]	2.43	1.18	1.99	4.35	1.45
	Rb [mg kg^{-1}]	0.508	0.409	0.7	0.9	0
	W [mg kg^{-1}]	0.39	0.371	0.48	0.75	0
	Zn [mg kg^{-1}]	5.72	0.943	5.63	6.91	4.71
Buried Ice	Ca [g kg^{-1}]	19.1	20.1	12.2	65.6	2.32
	Hg [g kg^{-1}]	1.13e-06	3.57e-06	0	1.13e-05	0
	Mg [g kg^{-1}]	5.65	5.79	3.44	19.1	0
	Rb [mg kg^{-1}]	0.15	0.255	0	0.651	0
	W [mg kg^{-1}]	0.0133	0.0421	0	0.133	0
	Zn [mg kg^{-1}]	6.5	5.53	6.86	18.1	0.493
Right Bank	Ca [g kg^{-1}]	7.37	6.09	5.12	21.8	0.78
	Hg [g kg^{-1}]	6.53e-07	2.53e-06	0	9.8e-06	0
	Mg [g kg^{-1}]	1.79	1.97	1.79	6.85	0
	Rb [mg kg^{-1}]	0.0153	0.0594	0	0.23	0
	W [mg kg^{-1}]	0.00733	0.0284	0	0.11	0
	Zn [mg kg^{-1}]	6.32	5.47	6.12	14.5	0.05
Tributary	Ca [g kg^{-1}]	4.85	5.11	1.8	14.6	0.97
	Hg [g kg^{-1}]	0.000423	0.000943	0	0.00255	0
	Mg [g kg^{-1}]	1.72	0.679	1.55	2.95	0.97
	Rb [mg kg^{-1}]	0.29	0.369	0	0.81	0
	W [mg kg^{-1}]	0.0229	0.0605	0	0.16	0
	Zn [mg kg^{-1}]	25.2	30.8	15	92.4	1.9

Table 6
Preliminary mean sediment source contributions to the riverbed and suspended (Phillips tube) target sediment samples (standard deviations in parentheses) and corresponding mean GOF based on the FingerPro software.

Sample	Distance from the glacier snout, km	Sediment source	Proportional contribution [%]	GOF [%]
1	0	Glacier	67.4 (20.8)	72
		Buried Ice	0.3 (2.5)	
		Right Bank	12.8 (18.8)	
		Tributary	19.5 (15.2)	
2	0.84	Glacier	57.2 (18.7)	78.3
		Buried Ice	36.1 (16.7)	
		Right Bank	6.3 (14.0)	
		Tributary	0.4 (1.7)	
3	1.62	Glacier	0.4 (3.4)	76.3
		Buried Ice	30.4 (31.2)	
		Right Bank	64.3 (32.8)	
		Tributary	4.9 (6.7)	
PT	1.62	Glacier	18.5 (12.4)	71.3
		Buried Ice	79.0 (15.1)	
		Right Bank	2.3 (8.5)	
		Tributary	0.1 (0.5)	

source appeared to be dominant for this sample, with an estimated contribution of 79% for this sample, while the "Glacier" source was estimated to be another substantial contributor (18.5%) (Table 6). Hence, the source fingerprinting suggests that on non-rainy days, the melting of buried ice, which is filled with fine sediment particles, is the primary sediment source. Although Koiavgan Creek also contributes to river water discharge at the catchment outlet, it is characterized by clean water on non-rainy days. The contribution (2.3%) of the "Right bank" source to the time-integrated suspended sediment also appeared to be negligible (Table 6).

5. Discussion

The assessment of sediment fluxes and sources in the Djankuat River catchment during the four years after the exceptional event on 1st July 2015 provides a basis for understanding the sediment dynamics of this catchment.

5.1. The magnitude of suspended sediment flux

In most cases, the hydrological regime of small glacierized rivers is characterized by a complete or almost complete absence of runoff during most of the year. 80–90% of water runoff and nearly 100% of sediment discharge occurs during the ablation season (Collins, 1996; Hasholt, 1996). However, variations in topography, altitude, precipitation distribution and the timing and volume of snowpack development and depletion lead to more complex hydrological regimes (Milano et al., 2015). Moreover, several researchers have found that climate change could alter both the magnitude and the timing of runoff events in such settings (Bibi et al., 2018; Zhong et al., 2018). To estimate the total annual sediment export, seasonal sediment export rates from this study were linearly extrapolated, considering that 98% of total runoff is discharged between May and September (Durgerov et al., 1972). On this basis, our estimated annual specific sediment yields ranged between 545 and 2467 $t \cdot km^{-2} \cdot yr^{-1}$ and varied significantly during the monitoring campaign (2015–2019). There is evidence of a negative trend (Table 3), which is likely associated with a reduced contribution of the "Right bank" sediment source due to a gradual decline of the riverbed and bank erosion in the newly formed Koiavgan Creek lower reach (Fig. 5).

The 5-year mean annual specific sediment yield estimate of 1118 $t \cdot km^{-2} \cdot yr^{-1}$ is 1.6 times higher than the corresponding value reported by Tsyplenkov et al. (2019) for high mountain catchments of the Caucasus (~700 $t \cdot km^{-2} \cdot yr^{-1}$). However, when excluding 2015, i.e. the year with the exceptional event, the average (2016–2019) annual sediment yield is 780 $t \cdot km^{-2} \cdot yr^{-1}$.

5.2. Suspended sediment source contributions: A geomorphic interpretation

We believe that the additional sediment input to the SY during the extreme rainfall events is associated with erosion of the Koiavgan Creek

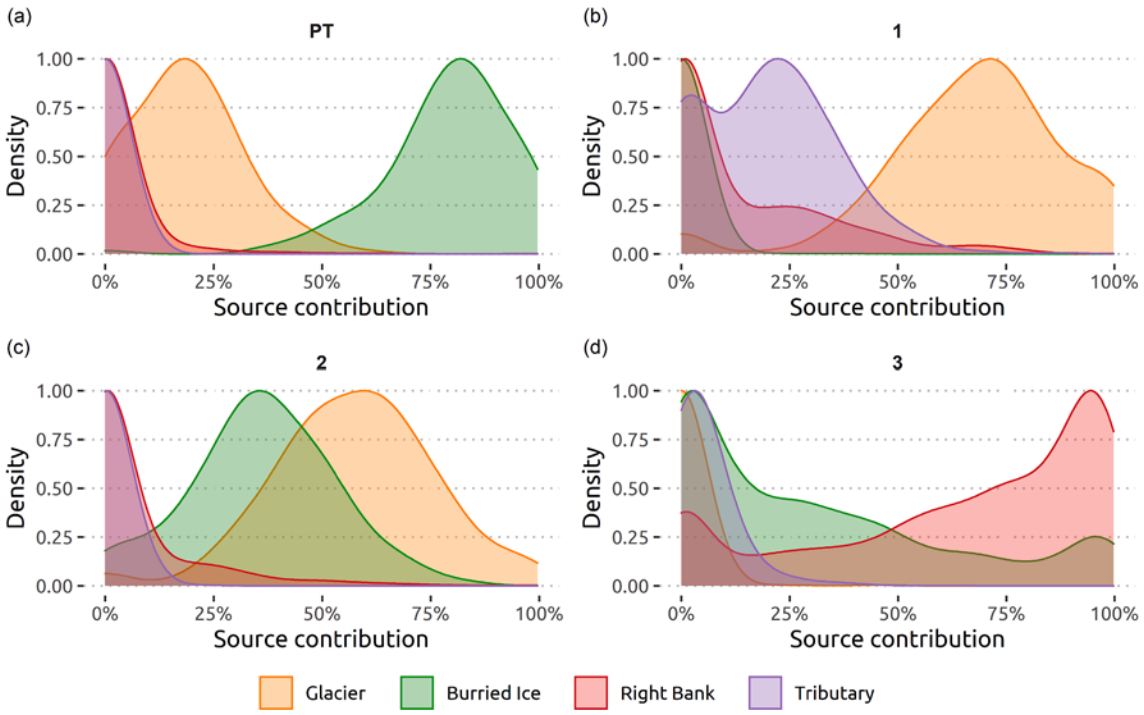

Fig. 7. Results of the un-mixing procedure for suspended sediment samples collected using the Phillips Tube (PT) (a) and riverbed target sediment samples (b–d). See Fig. 1 for sampling locations.

in the newly formed channel (in the reach crossing the lateral moraine in the area of the breakthrough), as well as the removal of fine material from the cone formed after the breakthrough (see Figs. 2 and 5). During rainstorms with <30 mm per day and non-rainy days, the water flow of the Koiavgan Creek does not lead to sediment transport (Tsyplenkov et al., 2020). This was confirmed by the results of detailed monitoring undertaken during August 2017 (see SM2). Moreover, there is almost no sediment cone in the Djankuat River valley bottom in the old Koiavgan Creek channel (see Figs. 1 and 4) which is an independent confirmation of the rather limited sediment supply from the "Tributary" and "Right bank" sediment sources before the breakthrough of the lateral moraine. As such, the exceptional event of 2015 considerably transformed the sediment redistribution pattern in the Djankuat River catchment. In the years following this event, it appears that every heavy rainfall event led to a sharp increase in sediment load (see Section 4.1), mainly due to the riverbed and bank erosion along the Koiavgan Creek channel in the reach of the lateral moraine breakthrough. Moreover, the removal of predominantly loose material due to the migration of the Koiavgan channel on the sediment cone most likely contributes considerably to the total sediment flux.

5.3. Preliminary application of the fingerprinting approach

The source apportionment estimates for the PT sample at the OUT sampling site provide data for a typical hydro-sedimentological response in September 2019 (melting without extreme rain) in the study catchment (Fig. 7a). These estimates suggest that the contribution of the proglacial zone ("Buried Ice" source) is about 79% (cf. Table 6) during such responses. This value corresponds well to those reported by other studies. For example, for a small river glacier in British Colombia, 80% of the sampled sediment load at the gauge was entrained from the proglacial area located 1.5 km below the snout (Orwin and Smart, 2004).

The timeline of the sediment fingerprinting estimates should be interpreted as follows. At the end of the melting season, the subglacial sediment supplies are exhausted. Such situations has been previously reported by many authors (Collins, 1990; Haritashya et al., 2006; Mao and Carrillo, 2017). In our case, the process of stagnant ice melting becomes the main contributor to the sediment yield of the Djankuat River on non-rainy days. This is reflected in the distribution of the probability density functions generated by FingerPro (cf. Fig. 7a). However, it is necessary to estimate the proportional contribution of "Glacier" and the other sediment sources to the SSL at the OUT gauging station using a PT for confirmation of this suggestion.

It is possible to conclude that, overall, the contribution of the "Tributary" sediment source is insignificant (cf. Figs. 7 and 8). The Koiavgan catchment is represented by a sizeable temporary sediment sink which is decoupled from the primary fluvial system. Some limited amounts of sediment can be delivered to the Djankuat River in the second half of the ablation season due to extreme rains. These are also typical features of many alpine catchments (Carrivick et al., 2013; Heckmann et al., 2018; Messenzehl et al., 2014).

The substantial contributions of both the "Tributary" and "Right bank" sediment sources to the bed sediments sampled near the glacier (see Fig. 8) are at first glance, surprising, given the target sediment sampling location (Sample 1). However, the predicted contributions from the "Tributary" and "Right bank" sediment sources are most likely a reflection of the connectivity beneath the main glacier.

The riverbed sediments in the high mountain river channel likely reflect the proportional contribution of various sediment sources during the last extreme flood (Fig. 8). It can be seen that near the glacier snout and even after the confluence with Koiavgan Creek, the "Glacier" is the main sediment source. The proglacial area ("Buried ice" sediment source) (see Figs. 2 and 8) is the second most important sediment source for the middle reach and outlet. The exceptionally high contribution of the "Right bank" at the catchment outlet is likely associated with erosion of the lower reach of the new Koiavgan channel and the new sediment cone (see Fig. 2). Both belong to the area represented by the "Right bank" sediment source (see Fig. 3). It is also possible that erosion of the right bank of the Djankuat in the section downstream of the confluence with the Koiavgan Creek was an important sediment source during the final stage of the flood.

The contribution of the "Right bank" sediment source became significant after the restructuring of the Koiavgan channel due to the lateral moraine breakthrough and the formation of a substantial sediment cone (1st July 2015). Before this exceptional event, the contribution of the "Right bank" was most likely limited, because of the partly protected slopes (by grasses) and the small drainage area of the sub-catchment.

5.4. Limitations and source fingerprinting reliability

In this study, we used a combination of research methods and techniques to assemble new insights into the impacts of extreme precipitation on sediment dynamics in a glacierized catchment experiencing a changing climate. Our intention in so doing, was to provide a weight-of-evidence interpretation of the findings. Inevitably, however, some limitations and uncertainties are associated with our work. First, we mainly focused on the suspended fraction of the sediment load. One would expect that the bedload component could represent a substantial proportion of the total load. Unfortunately, due to technical reasons, no bedload measurements were made during the field campaigns. Nonetheless, previous studies indicate that suspended sediment transport

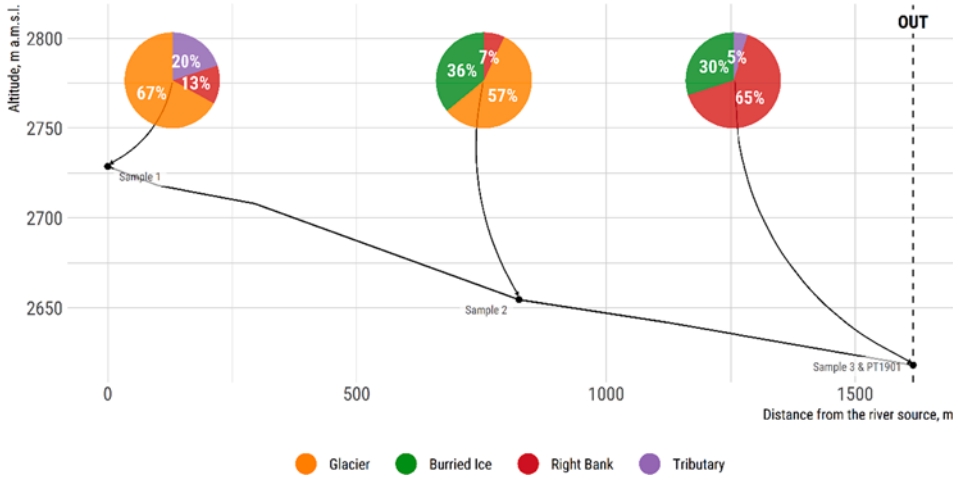

Fig. 8. Preliminary estimates of the proportional contributions from different sediment sources along the Djankuat River based on the fingerprinting results.

rates often correlate well with bedload transport rates, but may vary from flood to flood and year to year (Turowski et al., 2010). The average bedload proportion can be estimated with the help of partitioning tables classified by typical suspended sediment concentrations (Turowski et al., 2010). The mean SSC of the Djankuat River for the period 2015–2019 was 571 g·m^{-3}. Using this mean value, the partitioning table by Lane and Borland (1951) suggests 5–12% of the total sediment load would be bedload. A similar estimate (9–13%) is obtained when using the table from Williams and Rosgen (1989). However, the partitioning of the total sediment load is also controlled by the percentage of the catchment area that is glacierized (Turowski et al., 2010). Previously reported data on the bedload transport in glacierized catchments (Kjeldsen, 1977; 1975; Lauffer and Sommer, 1982) suggests that 11–23% of the total load is bedload for catchments that are 13–30% glacierized.

Furthermore, we acknowledge that the available data are insufficient to quantify the proportional contribution of the different sediment sources during and after the exceptional hydrological event. The source fingerprinting work was not planned in this manner and, additionally, the results should be seen as preliminary. Knowing the relative distribution of different grain sizes in the SSL of glacierized catchments (Bogen, 1989; Williams and Rosgen, 1989), we can hypothesize that the <63 μm fraction constitutes the majority of the suspended load of the Djankuat River. Therefore, it is possible that the preliminary information on the sources of the <63 μm fraction of the total load relates to >80% of the total sediment load and may therefore be a good indicator in terms of the total sediment output from the study catchment.

We also acknowledge that our preliminary source fingerprinting work combined the use of bed and suspended target sediment samples. This inevitably introduces uncertainties associated with particle size since we took a traditional approach of using the <63 μm fraction rather than measuring the particle size distributions of the samples. We recommend that future work measures the particle size fractions and explores the distribution of the tracer concentrations across the particle size distributions to select the most appropriate size fraction for direct comparisons between target sediment types and for minimizing uncertainties associated with particle size controls on tracers (Laceby et al., 2017). The use of channel bed sediment provided a pragmatic means of collecting material redeposited after floods caused by heavy rains and rapid glacier melting. A similar approach has been reported by many researchers working on mountain rivers (Haddadchi et al., 2014; Lepage et al., 2016). Riverbed sediments provide a basis for estimating source contributions during the ablation season and are, in essence, time-integrated to a degree. Since floodplains are not present in the upper reaches of most glacierized rivers, floodplain sediments cannot be used as an alternative to riverbed sediments. In other environmental settings, floodplain deposits have been used to provide a more long-term perspective on sediment source dynamics (Collins and Walling, 2004; Collins et al., 2017). The residence times of the bed sediment samples collected in this study were not investigated, and so there is no data to assess the direct comparability of bed sediment samples collected from different channel bars. The bed sediment samples were collected without the use of a stilling well since exposed material on point bars was sampled. This avoided the risk of losses of fines through winnowing but potentially introduced the risk of some alteration of the chemical signatures of the deposited material in conjunction with wetting and drying We also recommend future research collects suspended sediment and bed sediment samples at the same locations and at similar times under different flow conditions and sediment transport regimes. This will improve the consistency of the sampling strategy for source fingerprinting and increase the robustness of the results.

Our source tracing work used conventional elemental geochemistry but did not pre-select the tracers on the basis of their physico-chemical relevance to the study site nor their environmental behaviour. Our preliminary findings are, therefore, only based on a statistical solution using FingerPro. It would be useful to apply additional tracers in future work, and preferably those for which the physico-chemical suitability for the study site is better understood. FingerPro is a pragmatic tool for preliminary sediment source apportionment, but further work is needed to evaluate the reliability of the predicted source proportions arising from the un-mixing modelling. It uses a conventional GOF estimator, but this simply assesses the fit between predicted and measured tracer concentrations in the target sediment samples. It is well known that this GOF estimator frequently returns high values (Collins et al., 2020), although our results (Table 6) indicate that the errors associated with this approach are higher than those reported by many studies (Gaspar et al., 2019a; Laceby and Olley, 2015; Palazón et al., 2015). Importantly, we did not evaluate the preliminary estimates of the source proportions using either virtual or artificial mixtures, and this must be seen as another limitation. The wider evidence assembled by our mixed methods approach suggests, however, that the preliminary longitudinal source apportionment estimates are logical in the context of the connectivity beneath the glacier and the impact of the extreme event, resulting in the breakthrough of the lateral moraine. Our study suggests that fingerprinting can be used to assess the proportional contributions of various sediment sources in glacierized catchments experiencing extreme events. However, since our sourcing work has various limitations, our results should be interpreted with caution. On this basis, we have not directly integrated the preliminary source apportionment estimates with the measured suspended sediment fluxes.

Overall, we recommend further research in order to better quantitatively assess the sediment redistribution within the catchment, using available methods and approaches (Cavalli et al., 2013; Heckmann & Schwanghart, 2013; Messenzehl et al., 2014). In particular, extending the observation period and the temporal resolution of sediment fingerprinting is highly recommended.

5.5. *Wider implications of the study*

Our findings indicate that the proglacial zone (“Buried Ice”) and the “Glacier” are the primary sediment sources during days with little to average rainfall. However, the bank and riverbed erosion of the new lower reach of the Koiavgan Creek (i.e., the lateral moraine breakthrough area and the sediment cone formed after the 2015 exceptional event) are the main sediment sources during heavy rainfall events, contributing in total ~50% of the sediment yield of the Djankuat catchment in the first two years after the extreme event. This importance gradually declined during the next two years (due to a reduction in the incision rate of the new reach).

This is one of the first studies of suspended sediment loads in small glacierized river catchments in the Caucasus mountains, which are an essential element of the alpine mountain system of Eurasia, stretching from the European Alps to Tibet. As such, the results fill an important knowledge gap in assessing the impact of climate change on sediment discharge in the small proglacial rivers of the Caucasus mountains (Carrivick and Heckmann, 2017). The increase in the suspended sediment load of the Djankuat River is likely to continue for some time, given widely accepted projections for global warming this century (Hock et al., 2019). In particular, extreme events are likely to play an important role in this trend. The exceptional erosion event on the Djankuat River in 2015 removed in one day a volume of sediment, comparable to the annual sediment discharge. Measured SSCs reached up to 43,000 g m^{-3}, which is 3.5 times higher than the previously recorded maximum in glacial rivers (Haritashya et al., 2006). An even higher SSC (54,000 g m^{-3}) was recorded two years after this exceptional event, during a heavy rainstorm that led to the outburst of Lake Bashkara located in a neighbouring valley (Chernomorets et al., 2018). As such, this region of the Caucasus mountains is one of the world’s high-altitude areas, where glacier retreat contributes to a marked increase in suspended sediment loads (Carrivick and Heckmann, 2017; Hinderer et al., 2013).

6. Conclusion

The mean annual SY for 2015–2019 in the Djankuat proglacial river catchment increased to 1118 t km^{-2} yr^{-1} after the right-bank moraine breakthrough on 1st July 2015. This estimate is almost two times higher than other estimates for similar high mountain catchments of the Caucasus and one of the highest for proglacial rivers anywhere in the world. About 50% of sediment was exported by a limited number of extreme hydrological events (1–12% of the annual events), associated with heavy rainfalls. The frequency of such events is very likely to increase due to climate change. This may potentially lead to sediment loads from such high mountain catchments that are overall substantially higher in future decades compared to now.

A key sediment source explaining this increase was the new lower reach of the Koiavgan Creek channel (the right bank tributary) formed after the moraine breakthrough. This reach represents a crucial sediment source during events caused by heavy rainfall. However, this source's relative contribution is gradually declining as the incision rate of the new channel decreases. As a result, the sediment yield of the Djankuat also decreased from a minimum of 2467 t·km^{-2}·yr^{-1} in 2015 to 545 t·km^{-2}·yr^{-1} in 2019. We found that the area with "Buried Ice" is the main sediment source (79%) during non-rain days while the "Glacier" is the second most important source (21%). On days with light and moderate rains (daily precipitation < 30 mm), these contributions switched (i.e., "Glacier" — 67%, "Buried Ice" — 33%) in the uppermost study reach.

Future work should be undertaken to understand better the slope–river channel connectivity for the entire Djankuat River basin, paying particular attention to the Koiavgan Creek sub-catchment. The application of a fingerprinting technique, combined with traditional water discharge and turbidity observations herein, demonstrates promising results. However, the large spatio-temporal variations observed also indicate that regular and continued measurements are necessary to elucidate the evolving sediment dynamics fully. The combination of different monitoring and measurement techniques (e.g., sediment flux monitoring, geomorphic mapping and fingerprinting) can offer significant advantages in this regard.

Declaration of Competing Interest

The authors declare that they have no known competing financial interests or personal relationships that could have appeared to influence the work reported in this paper.

Data availability

Reproducible R code is available at the GitHub repository (https://github.com/atsyplenkov/djankuat-fingerptinting). Contact Anatoly Tsyplenkov (atsyplenkov@gmail.com) for more information.

Acknowledgements

This work was conducted with support from the ongoing Russian Science Foundation project No. 19-17-00181: "Quantitative assessment of the slope sediment flux and its changes in the Holocene for the Caucasus mountain rivers." This study contributes to the State Task no. 0148- 2019-0005, Institute of Geography RAS. Rothamsted Research receives funding from UKRI-BBSRC (UK Research and Innovation-Biotechnology and Biological Sciences Research Council), and the contribution to this manuscript by ALC was supported by the Soil to Nutrition institute strategic programme via grant award BBS/E/C/000I0330.

Funding

This study was funded by the project of the Russian Scientific Foundation (No 19-17-00181); the Soil to Nutrition institute strategic programme project 3 (BBS/E/C/000I0330).

Appendix A. Supplementary material

Supplementary data to this article can be found online at https://doi.org/10.1016/j.catena.2021.105285.

References

Bibi, S., Wang, L., Li, X., Zhou, J., Chen, D., Yao, T., 2018. Climatic and associated cryospheric, biospheric, and hydrological changes on the Tibetan Plateau: a review. Int. J. Climatol. 38, e1–e17. https://doi.org/10.1002/joc.5411.

Bogen, J., 1989. Glacial sediment production and development of hydro-electric power in glacierized areas. Ann. Glaciol. 6–11.

Carrivick, J.L., Geilhausen, M., Warburton, J., Dickson, N.E., Carver, S.J., Evans, A.J., Brown, L.E., 2013. Contemporary geomorphological activity throughout the proglacial area of an alpine catchment. Geomorphology 188, 83–95. https://doi.org/10.1016/j.geomorph.2012.03.029.

Carrivick, J.L., Heckmann, T., 2017. Short-term geomorphological evolution of proglacial systems. Geomorphology 287, 3–28. https://doi.org/10.1016/j.geomorph.2017.01.037.

Carrivick, J.L., Tweed, F.S., 2016. A global assessment of the societal impacts of glacier outburst floods. Glob. Planet. Change 144, 1–16. https://doi.org/10.1016/j.gloplacha.2016.07.001.

Cavalli, M., Trevisani, S., Comiti, F., Marchi, L., 2013. Geomorphometric assessment of spatial sediment connectivity in small Alpine catchments. Geomorphology 188, 31–41. https://doi.org/10.1016/j.geomorph.2012.05.007.

Cenderelli, D.A., Wohl, E.E., 2001. Peak discharge estimates of glacial-lake outburst floods and "normal" climatic floods in the Mount Everest region, Nepal. Geomorphology 40, 57–90. https://doi.org/10.1016/S0169-555X(01)00037-X.

Chernomorets, S.S., Petrakov, D.A., Aleynikov, A.A., Bekkiev, M.Y., Viskhadzhieva, K.S., Dokukin, M.D., Kalov, R.K., Kidyaeva, V.M., Krylenko, V.V., Krylenko, I.V., Krylenko, I.N., Rets, E.P., Savernyuk, E.A., Smirnov, A.M., 2018. The outburst of Bashkara glacier lake (Central Caucasus, Russia) on September 1, 2017 (In Russian). Kriosf. Zemli XXII 70–80. https://doi.org/10.21782/KZ1560-7496-2018-2(70-80).

Collins, A.L., Blackwell, M., Boeckx, P., Chivers, C.-A., Emelko, M., Evrard, O., Foster, I., Gellis, A., Gholami, H., Granger, S., Harris, P., Horowitz, A.J., Laceby, J.P., Martinez-Carreras, N., Minella, J., Mol, L., Nosrati, K., Pulley, S., Silins, U., da Silva, Y.J., Stone, M., Tiecher, T., Upadhayay, H.R., Zhang, Y., 2020. Sediment source fingerprinting: benchmarking recent outputs, remaining challenges and emerging themes. J. Soils Sediments 20, 4160–4193. https://doi.org/10.1007/s11368-020-02755-4.

Collins, A.L., Pulley, S., Foster, I.D.L., Gellis, A., Porto, P., Horowitz, A.J., 2017. Sediment source fingerprinting as an aid to catchment management: A review of the current state of knowledge and a methodological decision-tree for end-users. J. Environ. Manage. 194, 86–108. https://doi.org/10.1016/j.jenvman.2016.09.075.

Collins, A.L., Walling, D.E., 2004. Documenting catchment suspended sediment sources: problems, approaches and prospects. Prog. Phys. Geogr. Earth Environ. 28, 159–196. https://doi.org/10.1191/0309133304 pp409ra.

Collins, A.L., Walling, D.E., Leeks, G.J.L., 1997. Source type ascription for fluvial suspended sediment based on a quantitative composite fingerprinting technique. Catena 29, 1–27. https://doi.org/10.1016/S0341-8162(96)00064-1.

Collins, A.L., Walling, D.E., Leeks, G.J.L., 1996. Composite fingerprinting of the spatial source of fluvial suspended sediment : a case study of the Exe and Severn river basins, United Kingdom. Géomorphologie Reli. Process. Environ. 2, 41–53. https://doi.org/10.3406/morfo.1996.877.

Collins, D.N., 1996. Sediment transport from glacierized basins in the Karakoram mountains. IAHS Publ. Proc. Reports-Intern Assoc Hydrol. Sci. 236, 85–97.

Collins, D.N., 1990. Seasonal and annual variations of suspended sediment transport in meltwaters draining from an Alpine glacier. Hydrol. Mt. Reg. I, 439–446.

Cook, K.L., Andermann, C., Gimbert, F., Adhikari, B.R., Hovius, N., 2018. Glacial lake outburst floods as drivers of fluvial erosion in the Himalaya. Science (80-.). 362, 53–57. https://doi.org/10.1126/science.aat4981.

de Winter, I.L., Storms, J.E.A., Overeem, I., 2012. Numerical modeling of glacial sediment production and transport during deglaciation. Geomorphology 167–168, 102–114. https://doi.org/10.1016/j.geomorph.2012.05.023.

Dobriyal, P., Badola, R., Tuboi, C., Hussain, S.A., 2017. A review of methods for monitoring streamflow for sustainable water resource management. Appl. Water Sci. 7, 2617–2628. https://doi.org/10.1007/s13201-016-0488-y.

Durgerov, M.B., Freindlin, V.S., Chernova, L.P., 1972. Suspended sediment load in the Djankuat glacier basin during the summer of 1970 (In Russian). Mater. Glaciol. Issled. 19, 253–254.

Dyurgerov, M., 2003. Mountain and subpolar glaciers show an increase in sensitivity to climate warming and intensification of the water cycle. J. Hydrol. 282, 164–176. https://doi.org/10.1016/S0022-1694(03)00254-3.

Evans, S.G., Tutubalina, O.V., Drobyshev, V.N., Chernomorets, S.S., McDougall, S., Petrakov, D.A., Hungr, O., 2009. Catastrophic detachment and high-velocity long-runout flow of Kolka Glacier, Caucasus Mountains, Russia in 2002. Geomorphology 105, 314–321. https://doi.org/10.1016/j.geomorph.2008.10.008.

Evrard, O., Navratil, O., Ayrault, S., Ahmadi, M., Némery, J., Legout, C., Lefèvre, I., Poirel, A., Bonté, P., Esteves, M., 2011. Combining suspended sediment monitoring and fingerprinting to determine the spatial origin of fine sediment in a mountainous

river catchment. Earth Surf. Process. Landforms 36, 1072–1089. https://doi.org/10.1002/esp.2133.
Fryirs, K.A., Brierley, G.J., Preston, N.J., Kasai, M., 2007. Buffers, barriers and blankets: The (dis)connectivity of catchment-scale sediment cascades. Catena 70, 49–67. https://doi.org/10.1016/j.catena.2006.07.007.
Gaspar, L., Blake, W.H., Smith, H.G., Lizaga, I., Navas, A., 2019a. Testing the sensitivity of a multivariate mixing model using geochemical fingerprints with artificial mixtures. Geoderma 337, 498–510. https://doi.org/10.1016/j.geoderma.2018.10.005.
Gaspar, L., Lizaga, I., Blake, W.H., Latorre, B., Quijano, L., Navas, A., 2019b. Fingerprinting changes in source contribution for evaluating soil response during an exceptional rainfall in Spanish pre-pyrenees. J. Environ. Manage. 240, 136–148. https://doi.org/10.1016/j.jenvman.2019.03.109.
Goetz, J., Schwarz, C.J., 2020. fasstr: Analyze, Summarize, and Visualize Daily Streamflow Data.
Gurnell, A., 1995. Sediment yield from alpine glacier basins. In: Foster, I.D.L., Gurnell, A. M., Webb, B.W. (Eds.), Sediment and Water Quality in River Catchments. Wiley, Chichester, pp. 407–435.
Gurnell, A.M., 1987. Suspended Sediments. In: Gurnell, A.M., Clark, M.J. (Eds.), Glaciofluvial Sediment Transfer: An Alpine Perspective. Wiley & Sons, Chichester, pp. 305–354.
Guzmán, G., Quinton, J.N., Nearing, M.A., Mabit, L., Gómez, J.A., 2013. Sediment tracers in water erosion studies: current approaches and challenges. J. Soils Sediments 13, 816–833. https://doi.org/10.1007/s11368-013-0659-5.
Haddadchi, A., Nosrati, K., Ahmadi, F., 2014. Differences between the source contribution of bed material and suspended sediments in a mountainous agricultural catchment of western Iran. Catena 116, 105–113. https://doi.org/10.1016/j.catena.2013.12.011.
Haeberli, W., Huggel, C., Kääb, A., Zgraggen-Oswald, S., Polkvoj, A., Galushkin, I., Zotikov, I., Osokin, N., 2004. The Kolka-Karmadon rock/ice slide of 20 September 2002: an extraordinary event of historical dimensions in North Ossetia, Russian Caucasus. J. Glaciol. 50, 533–546. https://doi.org/10.3189/172756504781829710.
Harbor, J., Warburton, J., 1993. Relative Rates of Glacial and Nonglacial Erosion in Alpine Environments. Arct. Alp. Res. 25, 1. https://doi.org/10.2307/1551473.
Haritashya, U.K., Singh, P., Kumar, N., Gupta, R.P., 2006. Suspended sediment from the Gangotri Glacier: Quantification, variability and associations with discharge and air temperature. J. Hydrol. 321, 116–130. https://doi.org/10.1016/j.jhydrol.2005.07.037.
Harvey, A.M., 2012. The coupling status of alluvial fans and debris cones: a review and synthesis. Earth Surf. Process. Landforms 37, 64–76. https://doi.org/10.1002/esp.2213.
Hasholt, B., 1996. Sediment transport in Greenland. IAHS Publ. Proc. Reports-Intern Assoc Hydrol. Sci. 236, 105–114.
Hasholt, B., Walling, D.E., 1992. Use of caesium-137 to investigate sediment sources and sediment delivery in a small glacierized mountain drainage basin in eastern Greenland. In: Erosion, Debris Flows and Environment in Mountain Regions (Proceedings of the Chengdu Symposium, July 1992). IAHS Publ, pp. 87–100.
Hasholt, B., Walling, D.E., Owens, P.N., 2000. Sedimentation in arctic proglacial lakes: Mittivakkat Glacier, south-east Greenland. Hydrol. Process. 14, 679–699. https://doi.org/10.1002/(SICI)1099-1085(200003)14:4<679::AID-HYP966>3.0.CO;2-E.
Heckmann, T., Cavalli, M., Cerdan, O., Foerster, S., Javaux, M., Lode, E., Smetanová, A., Vericat, D., Brardinoni, F., 2018. Indices of sediment connectivity: opportunities, challenges and limitations. Earth-Sci. Rev. 187, 77–108. https://doi.org/10.1016/j.earscirev.2018.08.004.
Heckmann, T., Hilger, L., Vehling, L., Becht, M., 2016. Integrating field measurements, a geomorphological map and stochastic modelling to estimate the spatially distributed rockfall sediment budget of the Upper Kaunertal, Austrian Central Alps. Geomorphology 260, 16–31. https://doi.org/10.1016/j.geomorph.2015.07.003.
Heckmann, T., Schwanghart, W., 2013. Geomorphic coupling and sediment connectivity in an alpine catchment — Exploring sediment cascades using graph theory. Geomorphology 182, 89–103. https://doi.org/10.1016/j.geomorph.2012.10.033.
Hinderer, M., Kastowski, M., Kamelger, A., Bartolini, C., Schlunegger, F., 2013. River loads and modern denudation of the Alps — A review. Earth-Science Rev. 118, 11–44. https://doi.org/10.1016/j.earscirev.2013.01.001.
Hock, R., Rasul, G., Adler, C., Cáceres, B., Gruber, S., Hirabayashi, Y., Jackson, M., Kääb, A., Kang, S., Kutuzov, S., Milner, A., Molau, U., Morin, S., Orlove, B., Steltzer, H., 2019. High Mountain Areas. In: Pörtner, H.-O., Roberts, D.C., Masson-Delmotte, V., Zhai, P., Tignor, M., Poloczanska, E., Mintenbeck, K., Alegría, A., Nicolai, M., Okem, A., Petzold, J., Rama, B., Weyer, N.M. (Eds.), IPCC Special Report on the Ocean and Cryosphere in a Changing Climate.
Hoffmann, T., Müller, T., Johnson, E.A., Martin, Y.E., 2013. Postglacial adjustment of steep, low-order drainage basins, Canadian Rocky Mountains. J. Geophys. Res. Earth Surf. 118, 2568–2584. https://doi.org/10.1002/2013JF002846.
Huss, M., Farinotti, D., Bauder, A., Funk, M., 2008. Modelling runoff from highly glacierized alpine drainage basins in a changing climate. Hydrol. Process. 22, 3888–3902. https://doi.org/10.1002/hyp.7055.
Huss, M., Hock, R., 2018. Global-scale hydrological response to future glacier mass loss. Nat. Clim. Chang. 8, 135–140. https://doi.org/10.1038/s41558-017-0049-x.
Jennings, K.S., Winchell, T.S., Livneh, B., Molotch, N.P., 2018. Spatial variation of the rain–snow temperature threshold across the Northern Hemisphere. Nat. Commun. 9, 1148. https://doi.org/10.1038/s41467-018-03629-7.
Kharchenko, S., Tsyplenkov, A., Petrakov, D., Golosov, V., 2020. Causes and consequences of the streambed restructuring of the Koiavgan Creek (North Caucasus. Russia). E3S Web Conf. 163, 02003. https://doi.org/10.1051/e3sconf/202016302003.
Kjeldsen, O., 1977. Materialtransport Undersøkelser i Norske Breelver 1975. Technical Report 3–77.
Kjeldsen, O., 1975. Materialtransport Undersøkelser i Norske Breelver 1974. Technical Report 3–75.
Koiter, A.J., Owens, P.N., Petticrew, E.L., Lobb, D.A., 2013. The behavioural characteristics of sediment properties and their implications for sediment fingerprinting as an approach for identifying sediment sources in river basins. Earth-Science Rev. 125, 24–42. https://doi.org/10.1016/j.earscirev.2013.05.009.
Laceby, J.P., Evrard, O., Smith, H.G., Blake, W.H., Olley, J.M., Minella, J.P.G., Owens, P. N., 2017. The challenges and opportunities of addressing particle size effects in sediment source fingerprinting: A review. Earth-Science Rev. 169, 85–103. https://doi.org/10.1016/j.earscirev.2017.04.009.
Laceby, J.P., Olley, J., 2015. An examination of geochemical modelling approaches to tracing sediment sources incorporating distribution mixing and elemental correlations. Hydrol. Process. 29, 1669–1685. https://doi.org/10.1002/hyp.10287.
Lambert, C.P., Walling, D.E., 1988. Measurement of channel storage of suspended sediment in a gravel-bed river. CATENA 15, 65–80. https://doi.org/10.1016/0341-8162(88)90017-3.
Lana-Renault, N., Nadal-Romero, E., Serrano-Muela, M.P., Alvera, B., Sánchez-Navarrete, P., Sanjuan, Y., García-Ruiz, J.M., 2014. Comparative analysis of the response of various land covers to an exceptional rainfall event in the central Spanish Pyrenees, October 2012. Earth Surf. Process. Landforms 39, 581–592. https://doi.org/10.1002/esp.3465.
Lane, E.W., Borland, W.M., 1951. Estimating bed load. Trans. Am. Geophys. Union 32, 121. https://doi.org/10.1029/TR032i001p00121.
Lane, S.N., Bakker, M., Gabbud, C., Micheletti, N., Saugy, J.-N., 2017. Sediment export, transient landscape response and catchment-scale connectivity following rapid climate warming and Alpine glacier recession. Geomorphology 277, 210–227. https://doi.org/10.1016/j.geomorph.2016.02.015.
Lauffer, H., Sommer, N., 1982. Studies on sediment transport in mountain streams of the Eastern Alps. In: 14th International Congress on Dams, Rio de Janeiro, pp. 431–453.
Laute, K., Beylich, A.A., 2014. Environmental controls, rates and mass transfers of contemporary hillslope processes in the headwaters of two glacier-connected drainage basins in western Norway. Geomorphology 216, 93–113. https://doi.org/10.1016/j.geomorph.2014.03.021.
Leggat, M.S., Owens, P.N., Stott, T.A., Forrester, B.J., Déry, S.J., Menounos, B., 2015. Hydro-meteorological drivers and sources of suspended sediment flux in the pro-glacial zone of the retreating Castle Creek Glacier, Cariboo Mountains, British Columbia, Canada. Earth Surf. Process. Landforms 40, 1542–1559. https://doi.org/10.1002/esp.3755.
Lepage, H., Laceby, J.P., Bonté, P., Joron, J.L., Onda, Y., Lefèvre, I., Ayrault, S., Evrard, O., 2016. Investigating the source of radiocesium contaminated sediment in two Fukushima coastal catchments with sediment tracing techniques. Anthropocene 13, 57–68. https://doi.org/10.1016/j.ancene.2016.01.004.
Lewis, T., Braun, C., Hardy, D.R., Francus, P., Bradley, R.S., 2005. An Extreme Sediment Transfer Event in a Canadian High Arctic Stream. Arctic. Antarct. Alp. Res. 37, 477–482. https://doi.org/10.1657/1523-0430(2005)037[0477:AESTEI]2.0.CO;2.
Lizaga, I., Gaspar, L., Blake, W.H., Latorre, B., Navas, A., 2019. Fingerprinting changes of source apportionments from mixed land uses in stream sediments before and after an exceptional rainstorm event. Geomorphology 341, 216–229. https://doi.org/10.1016/j.geomorph.2019.05.015.
Lizaga, I., Latorre, B., Gaspar, L., Navas, A., 2018. fingerPro: An R package for sediment source tracing. https://doi.org/10.5281/zenodo.1402029.
Mabit, L., Benmansour, M., Walling, D.E., 2008. Comparative advantages and limitations of the fallout radionuclides 137Cs, 210Pbex and 7Be for assessing soil erosion and sedimentation. J. Environ. Radioact. 99, 1799–1807. https://doi.org/10.1016/j.jenvrad.2008.08.009.
Mao, L., Carrillo, R., 2017. Temporal dynamics of suspended sediment transport in a glacierized Andean basin. Geomorphology 287, 116–125. https://doi.org/10.1016/j.geomorph.2016.02.003.
Messenzehl, K., Hoffmann, T., Dikau, R., 2014. Sediment connectivity in the high-alpine valley of Val Müschauns, Swiss National Park — linking geomorphic field mapping with geomorphometric modelling. Geomorphology 221, 215–229. https://doi.org/10.1016/j.geomorph.2014.05.033.
Micheletti, N., Lane, S.N., 2016. Water yield and sediment export in small, partially glaciated Alpine watersheds in a warming climate. Water Resour. Res. 52, 4924–4943. https://doi.org/10.1002/2016WR018774.
Milano, M., Reynard, E., Bosshard, N., Weingartner, R., 2015. Simulating future trends in hydrological regimes in Western Switzerland. J. Hydrol. Reg. Stud. 4, 748–761. https://doi.org/10.1016/j.ejrh.2015.10.010.
Motha, J.A., Wallbrink, P.J., Hairsine, P.B., Grayson, R.B., 2003. Determining the sources of suspended sediment in a forested catchment in southeastern Australia. Water Resour. Res. 39 https://doi.org/10.1029/2001WR000794.
Navratil, O., Evrard, O., Esteves, M., Legout, C., Ayrault, S., Némery, J., Mate-Marin, A., Ahmadi, M., Lefèvre, I., Poirel, A., Bonté, P., 2012. Temporal variability of suspended sediment sources in an alpine catchment combining river/rainfall monitoring and sediment fingerprinting. Earth Surf. Process. Landforms 37, 828–846. https://doi.org/10.1002/esp.3201.
Orwin, J.F., Smart, C.C., 2004. Short-term spatial and temporal patterns of suspended sediment transfer in proglacial channels, small River Glacier. Canada. Hydrol. Process. 18, 1521–1542. https://doi.org/10.1002/hyp.1402.
Otto, J.-C., Schrott, L., Jaboyedoff, M., Dikau, R., 2009. Quantifying sediment storage in a high alpine valley (Turtmanntal, Switzerland). Earth Surf. Process. Landforms 34, 1726–1742. https://doi.org/10.1002/esp.1856.
Owens, P.N., Batalla, R.J., Collins, A.J., Gomez, B., Hicks, D.M., Horowitz, A.J., Kondolf, G.M., Marden, M., Page, M.J., Peacock, D.H., Petticrew, E.L., Salomons, W.,

Trustrum, N.A., 2005. Fine-grained sediment in river systems: environmental significance and management issues. River Res. Appl. 21, 693–717. https://doi.org/10.1002/rra.878.

Owens, P.N., Blake, W.H., Gaspar, L., Gateuille, D., Koiter, A.J., Lobb, D.A., Petticrew, E. L., Reiffarth, D.G., Smith, H.G., Woodward, J.C., 2016. Fingerprinting and tracing the sources of soils and sediments: Earth and ocean science, geoarchaeological, forensic, and human health applications. Earth-Science Rev. 162, 1–23. https://doi.org/10.1016/j.earscirev.2016.08.012.

Palazón, L., Latorre, B., Gaspar, L., Blake, W.H., Smith, H.G., Navas, A., 2015. Comparing catchment sediment fingerprinting procedures using an auto-evaluation approach with virtual sample mixtures. Sci. Total Environ. 532, 456–466. https://doi.org/10.1016/j.scitotenv.2015.05.003.

Phillips, J.M., Russell, M.A., Walling, D.E., 2000. Time-integrated sampling of fluvial suspended sediment: a simple methodology for small catchments. Hydrol. Process. 14, 2589–2602. https://doi.org/10.1002/1099-1085(20001015)14:14<2589::AID-HYP94>3.0.CO;2-D.

Pismenniy, A.N., Pichuzhkov, A.N., Zrubina, M.A., Gorbachev, S.A., Vertii, S.N., Grekov, I.I., Gamasa, Y.N., Tereschenko, L.A., 2013. State Geological Map of the Russian Federation. Scale 1:200,000; Sheet K-38-I—VII. VSEGEI Publishing House, Moscow, Russia.

Pulley, S., Collins, A.L., 2018. Tracing catchment fine sediment sources using the new SIFT (SedIment Fingerprinting Tool) open source software. Sci. Total Environ. 635, 838–858. https://doi.org/10.1016/j.scitotenv.2018.04.126.

Rainato, R., Mao, L., García-Rama, A., Picco, L., Cesca, M., Vianello, A., Preciso, E., Scussel, G.R., Lenzi, M.A., 2017. Three decades of monitoring in the Rio Cordon instrumented basin: Sediment budget and temporal trend of sediment yield. Geomorphology 291, 45–56. https://doi.org/10.1016/j.geomorph.2016.03.012.

Rets, E., Chizhova, J.N., Loshakova, N., Tokarev, I., Kireeva, M.B., Budantseva, N.A., Vasil'chuk, Y.K., Frolova, N., Popovnin, V., Toropov, P., Terskaya, E., Smirnov, A.M., Belozerov, E., Karashova, M., 2017. Using isotope methods to study alpine headwater regions in the Northern Caucasus and Tien Shan. Front. Earth Sci. 11, 531–543. https://doi.org/10.1007/s11707-017-0668-6.

Rets, E., Kireeva, M., 2010. Hazardous hydrological processes in mountainous areas under the impact of recent climate change: case study of Terek River basin. In: Global Change: Facing Risks and Threats to Water Resources. IAHS Publ 340, 126–134.

Rets, E.P., Popovnin, V.V., Toropov, P.A., Smirnov, A.M., Tokarev, I.V., Chizhova, J.N., Budantseva, N.A., Vasilchuk, Y.K., Kireeva, M.B., Ekaykin, A.A., Veres, A.N., Aleynikov, A.A., Frolova, N.L., Tsyplenkov, A.S., Poliukhov, A.A., Chalov, S.R., Aleshina, M.A., Kornilova, E.D., 2019. Djankuat glacier station in the North Caucasus, Russia: a database of glaciological, hydrological, and meteorological observations and stable isotope sampling results during 2007–2017. Earth Syst. Sci. Data 11, 1463–1481. https://doi.org/10.5194/essd-11-1463-2019.

Richardson, S.D., Reynolds, J.M., 2000. An overview of glacial hazards in the Himalayas. Quat. Int. 65–66, 31–47. https://doi.org/10.1016/S1040-6182(99)00035-X.

Rodda, H.J.E., Little, M.A., 2015. Understanding mathematical and statistical techniques in hydrology. John Wiley & Sons Ltd, Chichester, UK. https://doi.org/10.1002/9781119077985.

Sear, D.A., Lee, M.W.E., Oakley, R.J., Carling, P.A., Collins, M.B., 2002. Coarse sediment tracing technology in littoral and fluvial environments a review. In: Foster, I. (Ed.), Tracers in the Environment. Special Issue, Earth Surface Processes and Landforms. Wiley, pp. 21–55.

Shahgedanova, M., Popovnin, V., Aleynikov, A., Petrakov, D., Stokes, C.R., 2007. Long-term change, interannual and intra-seasonal variability in climate and glacier mass balance in the central Greater Caucasus, Russia. Ann. Glaciol. 46, 355–361. https://doi.org/10.3189/172756407782871323.

Shannon, S., Smith, R., Wiltshire, A., Payne, T., Huss, M., Betts, R., Caesar, J., Koutroulis, A., Jones, D., Harrison, S., 2019. Global glacier volume projections under high-end climate change scenarios. Cryosph. 13, 325–350. https://doi.org/10.5194/tc-13-325-2019.

Sloto, R.A., Crouse, M.Y., 1996. Hysep: a computer program for streamflow hydrograph separation and analysis. U.S. Geological Survey Water-Resources Investigations Report 96–4040.

Smith, H.G., Blake, W.H., 2014. Sediment fingerprinting in agricultural catchments: A critical re-examination of source discrimination and data corrections. Geomorphology 204, 177–191. https://doi.org/10.1016/j.geomorph.2013.08.003.

Stott, T.A., Mount, N.J., 2007. Alpine proglacial suspended sediment dynamics in warm and cool ablation seasons: Implications for global warming. J. Hydrol. 332, 259–270. https://doi.org/10.1016/j.jhydrol.2006.07.001.

Theler, D., Reynard, E., Lambiel, C., Bardou, E., 2010. The contribution of geomorphological mapping to sediment transfer evaluation in small alpine catchments. Geomorphology 124, 113–123. https://doi.org/10.1016/j.geomorph.2010.03.006.

Tsyplenkov, A., Vanmaercke, M., Golosov, V., 2019. Contemporary suspended sediment yield of Caucasus mountains. Proc. Int. Assoc. Hydrol. Sci. 381, 87–93. https://doi.org/10.5194/piahs-381-87-2019.

Tsyplenkov, A., Vanmaercke, M., Golosov, V., Chalov, S., 2020. Suspended sediment budget and intra-event sediment dynamics of a small glaciated mountainous catchment in the Northern Caucasus. J. Soils Sediments 20, 3266–3281. https://doi.org/10.1007/s11368-020-02633-z.

Turowski, J.M., Rickenmann, D., Dadson, S.J., 2010. The partitioning of the total sediment load of a river into suspended load and bedload: A review of empirical data. Sedimentology 57, 1126–1146. https://doi.org/10.1111/j.1365-3091.2009.01140.x.

Vezzoli, G., Garzanti, E., Limonta, M., Radeff, G., 2020. Focused erosion at the core of the Greater Caucasus: Sediment generation and dispersal from Mt. Elbrus to the Caspian Sea. Earth-Science Rev. 200, 102987 https://doi.org/10.1016/j.earscirev.2019.102987.

Walling, D.E., 2005. Tracing suspended sediment sources in catchments and river systems. Sci. Total Environ. 344, 159–184. https://doi.org/10.1016/j.scitotenv.2005.02.011.

Warburton, J., 1990. An alpine proglacial fluvial sediment budget. Geogr. Ann. Ser. A Phys. Geogr. 72, 261–272. https://doi.org/10.1080/04353676.1990.11880322.

Wichmann, V., Heckmann, T., Haas, F., Becht, M., 2009. A new modelling approach to delineate the spatial extent of alpine sediment cascades. Geomorphology 111, 70–78. https://doi.org/10.1016/j.geomorph.2008.04.028.

Williams, G.P., Rosgen, D.L., 1989. Measured total sediment loads (suspended loads and bedloads) for 93 United States streams. https://doi.org/10.3133/ofr8967.

Wilson, R., Harrison, S., Reynolds, J., Hubbard, A., Glasser, N.F., Wündrich, O., Iribarren Anacona, P., Mao, L., Shannon, S., 2019. The 2015 Chileno Valley glacial lake outburst flood, Patagonia. Geomorphology 332, 51–65. https://doi.org/10.1016/j.geomorph.2019.01.015.

Yermolaev, O.P., Sharifullin, A.G., Golosov, V.N., Safarov, K.N., 2015. Recent Exogenous Processes in Mountain Landscapes of the Temperate Zone of Northern Eurasia and Assessment of Their Contribution to the Sediment Load of Rivers Using Satellite Data. Uchenye Zap. Kazan. Univ. Seriya Estestv. Nauk. 2, 81–93 (In Russian).

Zemp, M., Hoelzle, M., Haeberli, W., 2009. Six decades of glacier mass-balance observations: a review of the worldwide monitoring network. Ann. Glaciol. 50, 101–111. https://doi.org/10.3189/172756409787769591.

Zhong, R., He, Y., Chen, X., 2018. Responses of the hydrological regime to variations in meteorological factors under climate change of the Tibetan plateau. Atmos. Res. 214, 296–310. https://doi.org/10.1016/j.atmosres.2018.08.008.